

Enhancement of photocatalytic activity of ZnO–SiO₂ by nano-sized Pt for efficient removal of dyes from wastewater effluents

Leila Vafayi*, Soodabe Gharibe

Department of Science, Firoozkooh Branch, Islamic Azad University, Firoozkooh, Iran.

Received 25 February 2015; received in revised form 13 April 2015; accepted 17 May 2015

ABSTRACT

In this work, ZnO/SiO₂ nanoparticles were prepared using sol-gel method, and platinum particles were loaded on ZnO/SiO₂ nanoparticles by photoreductive method. Samples were characterized by X-ray diffraction (XRD), scanning electron microscopy (SEM) and Fourier transform infrared spectroscopy (FT-IR). The XRD patterns showed that the zinc oxide samples have a wurtzite structure (hexagonal phase). The crystallite size calculated by Scheerer's equation is ~ 32 nm. For photocatalytic test, decomposition of Rhodamine B (RB), as an organic pollutant, was carried out. A comparison of degradation between bare catalyst and platinum loaded ZnO/SiO₂ nanoparticle under UV-Vis light irradiation shows that the Pt- ZnO/SiO₂ photocatalyst is more efficient than ZnO/SiO₂ nanoparticles. Also, the activity of ZnO/SiO₂ nanoparticles in the visible light are minimal, while loading of Pt in zinc oxide network displaced the band gap toward longer wavelengths (visible light) and improved the photocatalysis activity of ZnO/SiO₂ in the range of visible light.

Keywords: Photocatalyst; Rhodamine B; UV-Vis; ZnO; Organic pollutants.

1. Introduction

Dyestuffs are a ubiquitous class of synthetic organic pigments that represent an increasing environmental danger. Within the overall category of dyestuffs, Rhodamine B is one of the most important xanthene dyes. Rhodamine B has a lot of applications. It has been used in paper and dye lasers. Owing to its extensive usage, it has become a common organic pollutant. Thus the photodegradation of Rhodamine B is important with regard to the purification of dye effluents [1]. Therefore, the dye degradation has been studied by using different procedures such as biological treatment, incineration and advanced oxidation processes [2–5].

Elimination of persistent organic pollutants that remain for a long time in the environment is one of the most difficult processes of the effluent treatment. Many methods are employed to remove or destroy the pollutants of effluents and contaminating gases. Some destructive methods use strong oxidants which are harmful.

On the other hand, currently used non-destructive methods can result in some serious problems. For example, air stripping which is (a method for the removing the volatile organic compounds from surface water or groundwater) converts water contamination to the air pollution. Additionally, carbon adsorption used for produces a harmful solid which should be destroyed. One of the weaknesses of these old processes is that the pollutants are not destroyed, but displaced from one phase to another. Therefore, methods for destruction of organic pollutants should be replaced with methods exerting less or negligible harms on the environment [6-11].

Low reaction rate of metallic oxides photocatalysis in the degradation reactions has necessitated the synthesis of new photocatalysts. Thus, many researchers tried to optimize different properties such as crystalline structure, particle size, band gap, surface area, and different beds. Synthesis of nano-size particles is a method to increase the surface area of a photocatalyst to increase the reactive sites on its surface to be increased. In order to increase the active centers of a catalyst, it can be covered on a stabilizer such as silica [12-15].

*Corresponding author email: leilavafayi@yahoo.com
Tel: +98 21 7644 3869; Fax: +98 21 7644 2868

The use of ultraviolet light for destroying pollutants by photocatalysts is a limitation for industry. Since the photocatalysts are semiconductor, this problem can be overcome by reducing the band gap. A method for reducing the band gap is to dope metals such as platinum, vanadium, silver *etc.* into the structure of photocatalysts [16-21].

In this work, the preparation results of two nano-photocatalysts: ZnO/SiO₂ and Pt-ZnO/SiO₂ have been reported [22]. Also, the photocatalytic decomposition of Rhodamine B as an organic dye pollutant using two photocatalysts under UV-Vis light irradiation has been investigated.

2. Experimental

All materials used in this work were purchased from Merck and used without modification.

2.1. Preparation of ZnO nanoparticles

In a typical synthesis, a solution of 5 mmol zinc acetate dihydrate in 30 mL absolute ethanol was added to a solution of surfactant CTAB (Zn(Ac)₂.2H₂O to CTAB molar ratio was equal to 1) in 30 mL of absolute ethanol under stirring. In order to obtain the pH value of ~10 in solutions, 20 mL of NaOH (0.3M) solution was added to the above solution under continuous stirring. The new solution was kept in a water bath at 70 °C for 2 h. It was observed that the solution started precipitating after one hour in water bath. After cooling the system to room temperature, the product was separated by centrifugation, washed with absolute ethanol and deionized water for several times. The powder was dried under vacuum at 70 °C for 10 h. Finally, the nanoparticles were calcined at 750 °C for 3 h.

2.2. Preparation of nano-photocatalyst ZnO/SiO₂

pH of 20 ml of a suspension containing 0.01 mole ZnO was adjusted to 9-10 by adding NaOH solution (0.3 M). This mixture refluxed after severe stirring for 10 h at 70 °C until stable zinc hydroxide sols were formed. After the reflux was finished, some tetraethyl orthosilicate was dropped on the sol at the same temperature to achieve the mole ratio of 30/70 (zinc/silicon). The formed sol was kept in the vacuum at room temperature for two days. Then it was calcined at 400 °C for 3 h.

2.3. Preparation of Pt-loaded ZnO/SiO₂

5 mmol ZnO/SiO₂ were stirred in 50 mL of methanol aqueous solution (1%wt) containing 1 mL of H₂PtCl₆ solution (0.4M) and irradiated by two 30 W Hg lamp for 20 h. During the irradiation, H₂PtCl₆ was photoreduced to disperse Pt metal particles over ZnO/SiO₂ catalysts to form Pt-loaded (1 wt %) ZnO/SiO₂. After filtering and washing distilled water,

the photocatalysts were dried at 200 °C for 2 h to remove the excess methanol adsorbed on the catalysts surface.

2.4. Degradation of Rhodamine B dye using the synthesized catalysts

Suspensions containing 150 ml of 10 ppm Rhodamine B dye together with ZnO/SiO₂ and Pt-ZnO/SiO₂ catalysts with different concentrations of 0.2, 0.3, and 0.4 g/L (pH of the suspensions was stabilized at 3, 4, 5, and 6), a magnetic stirrer, and an air flow which was blown into a reactor through a tube to uniform the environment were used in each experiment. The reactor consisted of two tungsten lamps; those with wavelength of 220-230 nm was used for irradiation at UV range and those with wavelength of 500-700 nm for irradiation at visible range.

In order to optimize the amount of catalyst and the environment pH, the irradiation time was set to 120 min.

Before irradiation, all solutions were stirred for 30 min in the dark to balance absorption and desorption of pollutants on the catalyst surface. A UV-Vis spectrophotometer was used to study the degradation of pollutants. Thus the absorption spectra of the samples were measured at certain intervals and the amount of pollutant removal or its conversion to another substance was evaluated by decrease in intensity of the relevant absorption peak.

2.5. Characterization

The crystal phase and particle size of the synthesized products were characterized by X-ray diffraction (XRD) using FK60-04 with Cu K α radiation ($\lambda = 1.54$ Å), and with instrumental setting of 35 kV and 20 mA. The morphology of the nanostructures was observed by emission scanning electron microscopy (SEM, PHILIPS-XL ϕ 30). Fourier transform infrared (FT-IR) spectra were recorded by SHIMADZU-840S spectrophotometer using KBr pellet. BET analysis was carried out with QUANTASORB. UV-Vis Diffuse Reflectance Spectra (DRS) were obtained for the dry-pressed disk samples using a UV-Vis spectrophotometer (SHIMADZU-2550). The amount of degradation of Rhodamine B was investigated by measuring the adsorption intensity of remained Rhodamine B in the solution by means of UV-Vis spectroscopy (SHIMADZU-2550).

3. Results and Discussion

3.1. Structural analysis of the catalysts

The XRD patterns of bare ZnO nanoparticles (a), ZnO@SiO₂ (b) and Pt-loaded ZnO/SiO₂ nanophotocatalysts (c) are shown in Fig. 1 (a-c). All peaks can be well indexed to wurtzite type crystal structure (hexagonal phase) with lattice constants of

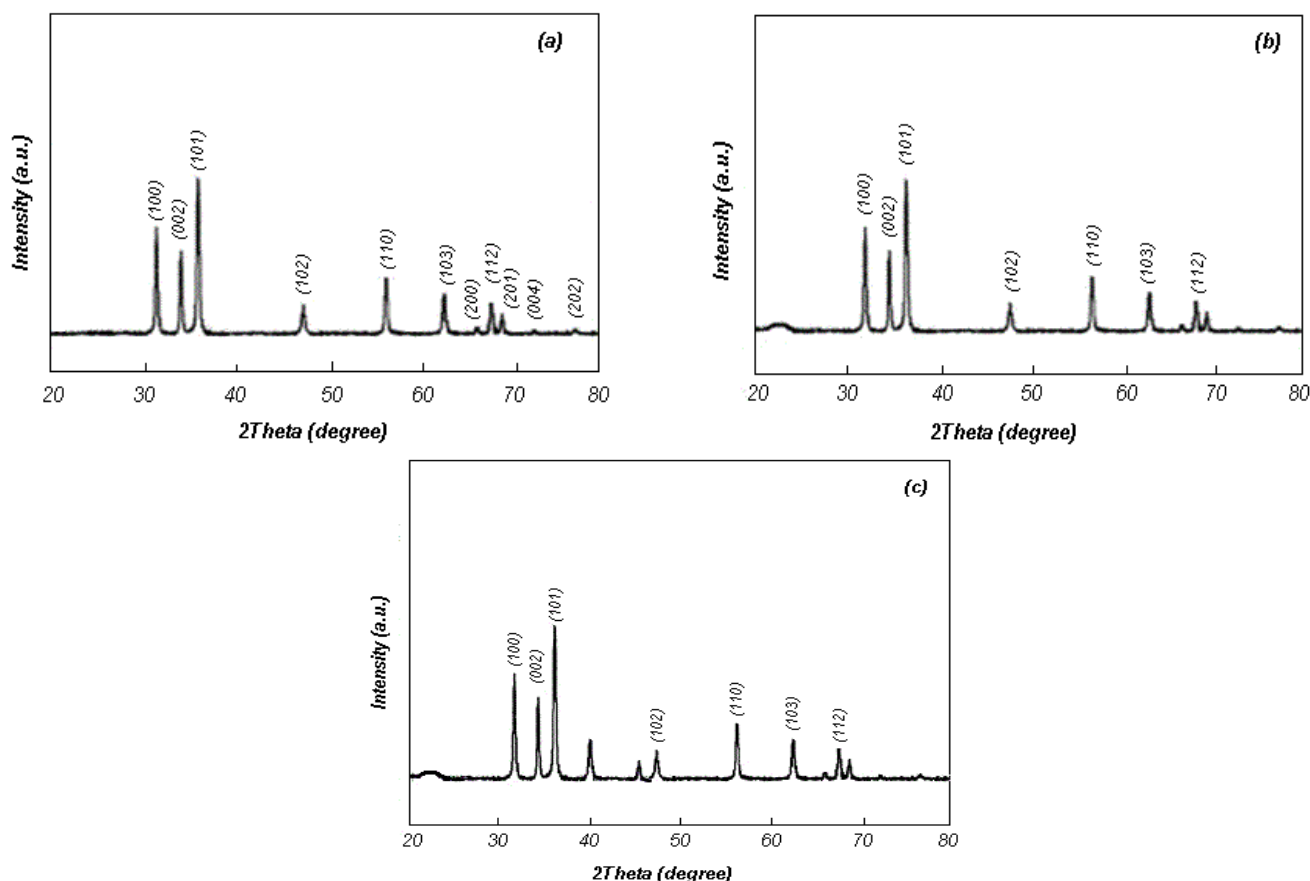


Fig. 1. XRD patterns of (a) ZnO, (b) ZnO/SiO₂, and (c) Pt - ZnO/SiO₂ samples.

$a=0.32495$ nm and $c=0.52069$ nm (JCPDS, No. 36-1451) [22,23]. No other crystalline phases were found in the XRD patterns, indicating the high purity of the products.

The crystallite sizes can be calculated using Scherrer's equation: $D = 0.9 \lambda / (\beta \cos\theta)$ where λ is the X-ray wavelength (1.54\AA), β is the full-width at half-maximum intensity of the diffraction line and θ is the diffraction angle. The crystallites sizes are estimated to be around 32 nm. Also the surface area of $358 \text{ m}^2/\text{g}$ was obtained for ZnO catalyst calcined at 750°C temperature from BET analysis.

In Fig. 1b a broad new peak is appeared at $\sim 22^\circ$, diffraction angle, which shows the presents of amorphous SiO₂ in the sample [22,23]. Fig. 1c shows the XRD pattern of Pt doped ZnO/SiO₂ sample. In Fig. 1c two new peaks are appeared at 40.05° and 46.52° diffraction angles, which can be well indexed to platinum (JCPDS, No. 01-1194). Therefore it can be concluded that the Pt-loaded ZnO/SiO₂ is carried out successfully.

The FT-IR spectra of ZnO and ZnO/SiO₂ nanoparticles are shown in Fig. 2(a-b).

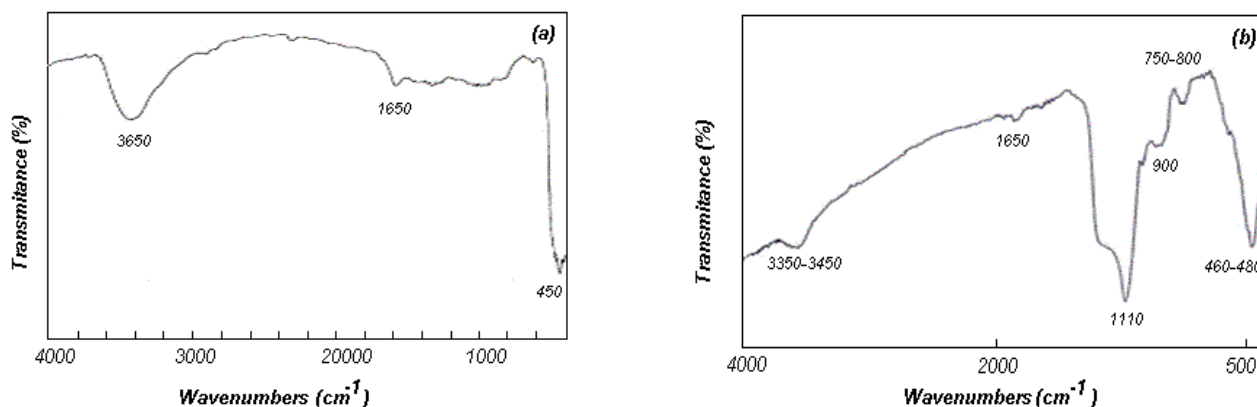


Fig. 2. FT-IR spectra of (a) ZnO and (b) ZnO/SiO₂ samples.

The vibrational peaks in the range of $3600\text{-}3650\text{ cm}^{-1}$ and $1600\text{-}1650\text{ cm}^{-1}$ can be attributed to the stretching and bending vibrations of structural hydroxyl groups of the adsorbed water. The peak in the range of $420\text{-}450\text{ cm}^{-1}$ can be associated to the stretching vibration mode of Zn-O [24-26]. The peaks in the ranges of $1050\text{-}1110\text{ cm}^{-1}$ and $750\text{-}800\text{ cm}^{-1}$ in Fig. 2b are corresponded to the asymmetric and symmetric stretching vibration modes of Si-O-Si, respectively, however these peaks are absent in Fig. 2a. The peak which is appeared at $440\text{-}480\text{ cm}^{-1}$ is due to the bending vibration mode of Si-O-Si [27,28]. These results are in agreement with the results of XRD patterns.

The morphology of the products was observed by SEM images. The SEM images of ZnO, and Pt-doped ZnO/SiO₂ nanoparticles are shown in Fig. 3 (a-b), respectively.

3.2. Photocatalytic activity

3.2.1. Degradation of Rhodamine B dye using ZnO/SiO₂ and Pt-ZnO/SiO₂ photocatalysts under UV irradiation

Rhodamine B dye has three absorption bands at wavelengths of 522, 352, and 224 nm. These bands are related to $\pi \rightarrow \pi^*$ transformation of the aromatic ring induced by N-ethyl groups attached to them.

The two other bands (352 and 224 nm) also refers to $n \rightarrow \sigma^*$ and $\sigma \rightarrow \sigma^*$ transformation of the aromatic ring, respectively (Fig. 4). The mechanism of Rhodamine B dye degradation proceeds through either conjugated structure degradation or diethyl removal. The decrease in the absorption intensity during the diethyl removal reaction is associated with a shift of the absorption peak (522 nm) toward shorter wavelengths. During degradation, the gradual elimination of *N,N*-diethyl chromophore which is an electron donor results in the absorption range of aromatic system to shift toward shorter wavelengths. However, if the maximum peak intensity gradually decreases without any shift in the absorption wavelength, the reaction proceeds through the conjugated structure degradation [29].

Figs. 4-7 show the degradation of Rhodamine B dye at pH range of 3-6 on ZnO/SiO₂ (0.3 g/L). As seen in the general pattern of the spectra, the absorption amount of Rhodamine B dye on this catalyst is directly related to the pH increment. This behaviour is due to the fact that at pH below pH_{zcp} (8.7) the catalyst surface is positively charged, thus it has more potential to attract negatively charged ions. By increasing pH and its approaching to pH_{zcp} , negative charges are gradually increased on the catalyst surface. Therefore, Rhodamine B dye with an unstable positive charge is better absorbed by the catalyst.

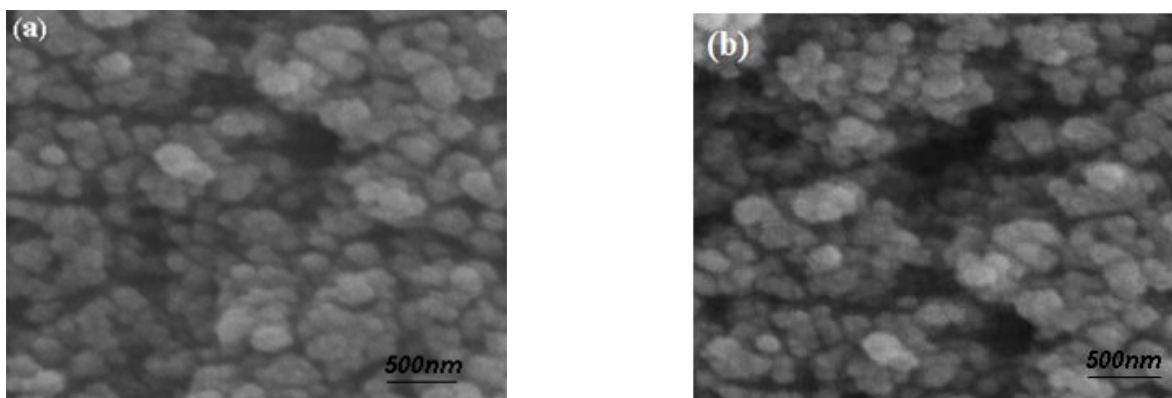


Fig. 3. SEM images of (a) bare ZnO, and (b) Pt- ZnO/SiO₂ nanoparticles.

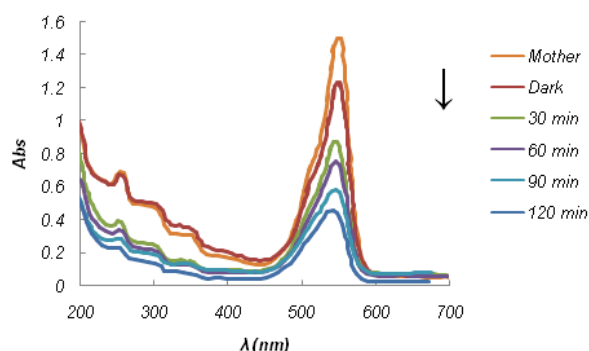


Fig. 4. Photodegradation of RB on bare ZnO/SiO₂ photocatalyst at pH=3.

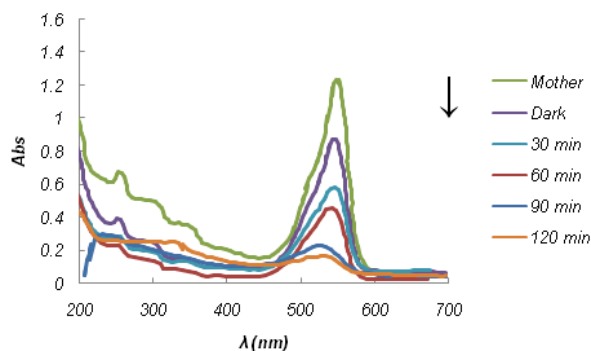


Fig. 5. Photodegradation of RB on bare ZnO/SiO₂ photocatalyst at pH=4.

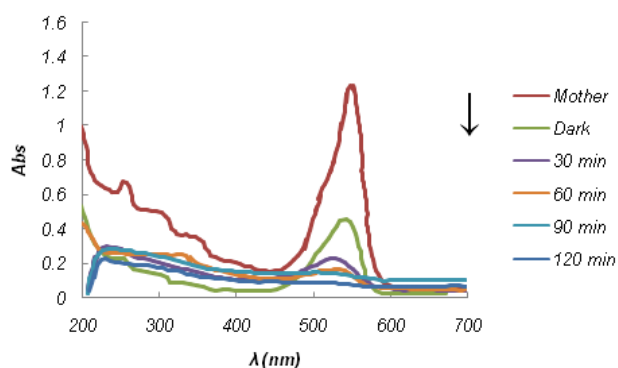


Fig. 6. Photodegradation of RB on bare ZnO/SiO₂ photocatalyst at pH=5.

Besides the progress of degradation reaction, decrease of intensity in the absorption peak with maximum intensity without any shift in the absorption wavelength is observed in all UV-Vis absorption spectra (Figs. 4-7). As mentioned earlier, if the maximum peak intensity gradually decreases without any shift in the absorption wavelength, the reaction proceeds through the conjugated structure degradation.

At pH = 5, the peaks are completely disappeared after two hours. According to the degradation reactions of Rhodamine B in the presence of ZnO/SiO₂ (0.3 g/L) at pH= 3-6, the highest photocatalytic activity of ZnO/SiO₂ was obtained at pH =5. The optimum amount of ZnO/SiO₂ and appropriate pH of the solution for degradation of 150 ml Rhodamine B dye with a concentration of 10 ppm were obtained 0.3 g/L and 5, respectively, (Tables 1 and 2).

Table 1. The results of photodegradation of RB (%) on ZnO/SiO₂ photocatalyst (0.2, 0.3 and 0.4 g/L) at pH=5.

The amount of ZnO/SiO ₂ (g/L), pH=5	The degradation of RB (%)
0.2	72.5
0.3	100
0.4	74.3

Table 2. The results of photodegradation of RB (%) on ZnO/SiO₂ photocatalyst (0.3 g/L) at pH=3, 4, 5, and 6.

pH (The amount of ZnO/SiO ₂ = 0.3 g/L)	The degradation of RB (%)
3	22.4
4	63.3
5	100
6	70.2

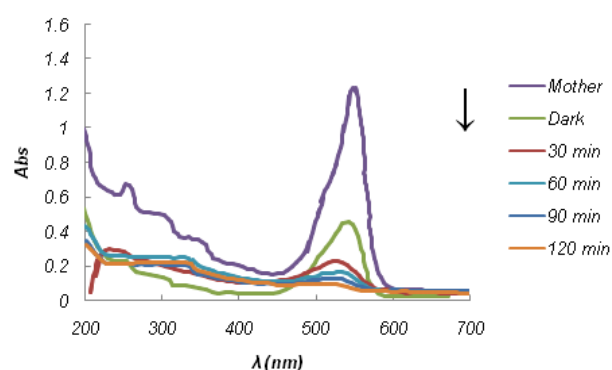


Fig. 7. Photodegradation of RB on bare ZnO/SiO₂ photocatalyst at pH=6.

Fig. 8 shows the variation of Rhodamine B spectrum treated through heterogeneous photocatalysis with 0.3 g/L Pt-ZnO/SiO₂ at pH= 5 (optimal conditions) for 90 minutes. The decreasing of the maximum peak absorption intensity and the variation of dye concentration are quite obvious from the spectra. As seen, the absorption initial amount of the dye is more in this catalyst than ZnO/SiO₂, while UV-Vis spectra pattern of both pure and doped catalysts are like each other. Higher dye adsorption in Pt-ZnO/SiO₂ is due to the low pH_{zcp} of this catalyst (4.2). In addition, alteration of the dye concentration from spectra shows that the destructive reaction of Rhodamine B on Pt-ZnO/SiO₂ occurs faster than ZnO/SiO₂ under UV irradiation. This behaviour is related to the presence of platinum. As we know, doped metal ions affect optical activity through trapping electrons or holes and altering the reproduction rate of e⁻/h⁺ [30].

3.2.2. Degradation of Rhodamine B dye with ZnO/SiO₂ and Pt-ZnO/SiO₂ photocatalysts under visible light

Since ZnO/SiO₂ has a large band gap, it is not able to perform photocatalysis reaction in the visible light. The band gap of ZnO/SiO₂ and Pt-ZnO/SiO₂ were calculated by UV-Vis diffuse reflectance spectra (Fig. 10) and equation 1.

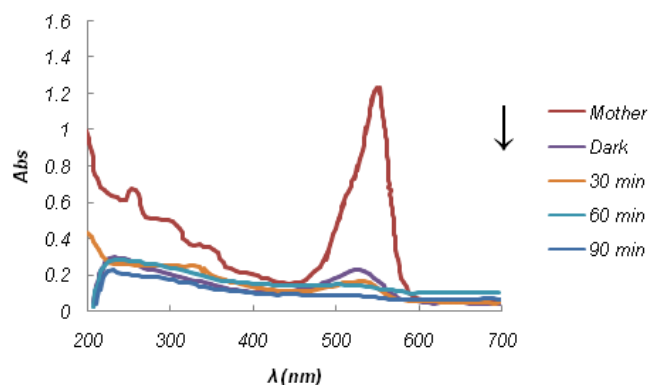


Fig. 8. Photodegradation of RB on Pt-ZnO/SiO₂ photocatalyst at pH=5.

The band gap values are obtained around 3.20 and 2.19 eV for ZnO/SiO₂ and Pt-ZnO/SiO₂, respectively.

$$E = hc / \lambda \quad (1)$$

Where λ is estimated from shoulder or peak of the spectra correspond to the fundamental absorption edges in the samples. h is Planck constant, c is the speed of light and E is energy ($1\text{eV} = 1.602 \times 10^{-19}\text{ J}$).

Fig. 9 shows changes in the absorption spectra of Rhodamine B by Pt-ZnO/SiO₂ under visible light. As seen in this figure, changes in the absorption spectra of Rhodamine B catalyst by Pt-ZnO/SiO₂ under visible light are similar to the degradation mechanism under UV radiation. The reaction is continued for about 120 min and Rhodamine B is completely degraded by Pt-ZnO/SiO₂ under visible light. Owing to the band gap distance of ZnO/SiO₂ (3.20 eV), the activity of ZnO/SiO₂ in the visible light is minimal. However, while doping of Pt in ZnO network displaced the band gap toward longer wavelengths (visible light) and increases the photocatalysis activity in the range of visible light. UV-Vis diffuse reflectance spectra of catalysts (Fig. 10) confirms the decrease of Pt-ZnO/SiO₂ band gap compared to ZnO/SiO₂.

4. Conclusions

ZnO/SiO₂ nanocomposite was prepared using sol-gel method, and platinum particles were successfully loaded on this nano-photocatalyst by photoreductive method. The results were found that the amount of adsorbed Rhodamine B dye on this catalyst is directly related to the pH increment. The optimum amount of ZnO/SiO₂ and appropriate pH of the solution for degradation of 150 ml Rhodamine B dye with a concentration of 10ppm were obtained 0.3 g/L and 5, respectively. In optimal conditions, alteration of the dye concentration from spectra shows that the destructive reaction of Rhodamine B on Pt-ZnO/SiO₂ occurs faster than ZnO/SiO₂ under UV irradiation. Moreover, the activity of ZnO/SiO₂ in the visible light

is minimal, while doping of Pt in ZnO network displaced the band gap toward longer wavelengths (visible light) and increased the photocatalysis activity in the range of visible light. The results of the photocatalytic test reveal that Pt-ZnO/SiO₂ may be an extremely viable adsorbent for application in the treatment of water and industrial wastewater contaminated with dyes.

Acknowledgment

This article was extracted from the project entitled: "Doping of Pt on ZnO/SiO₂ and Photodegradation of industrial wastewaters by Pt-ZnO/SiO₂ Nanophotocatalyst". Financial support for this project was provided by Islamic Azad University Firoozkooh branch.

References

- [1] Y. Ma, J.N. Yao, J. Photochem. Photobiol. A 116 (1998) 167-170.
- [2] A.M. Luis, M.C. Neves, M.H. Mendonc, O.C. Monteiro, Mater. Chem. Phys. 125 (2011) 20-25.
- [3] J.J. Lopez-Penalver, M. Sanchez-Polo, C.V. Gomez-Pacheco, J. Rivera-Utrilla, J. Chem. Technol. Biotechnol. 85 (2010) 1325-1333.
- [4] S. Sontakke, J. Modak, G. Madras, Chem. Eng. J. 165 (2010) 225-233.
- [5] E.G.L. Oliveiraa, J.J. Rodrigues. H.P. de Oliveiraa, Chem. Eng. J. 172 (2011) 96-101.
- [6] M.A. Fox, M.T. Dulay, Chem. Rev. 93 (1993) 341-357.
- [7] H. Shu, J. Xie, H. Xu, H. Li, Z. Gu, G. Sun, Y. Xu, J. Alloy. Compd. 496 (2010) 633-637.
- [8] G.K. Pradhan, K.M. Parida, Int. J. Eng. Sci. Technol. 2 (2010) 53-65.
- [9]. N. P. Mohabansi, V. B. Patill, N. Yenkie, R. Rasayan, J. Chem. 4 (2011) 814-819.
- [10] R. Slama, F. Ghribi, A. Houas, C. Barthou, L.E. Mir, Int. J. Nanoelect. Mater. 3 (2010)133-142.
- [11] A. F. Comanescu, M. Mihaly, A. Meghea, UPB. Sci. Bull. Series B 74 (2012) 49-60.

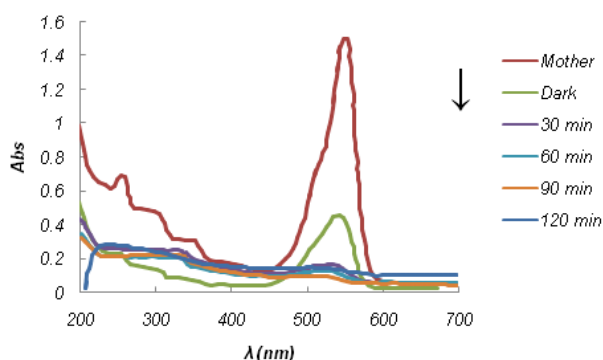


Fig. 9. Photodegradation of RB on Pt-ZnO/SiO₂ photocatalyst at pH=5 (under visible light).

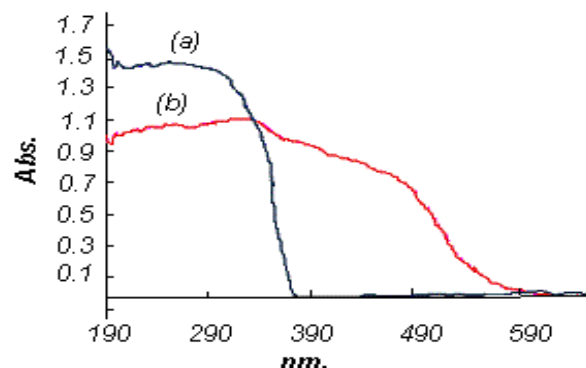


Fig. 10. UV-Vis Diffuse Reflectance Spectra of (a) ZnO/SiO₂, and (b) Pt-ZnO/SiO₂ nanoparticles.

- [12] D.V. Demydov, Nanosized Alkaline Earth Metal Titanates: Effects of Size on Photocatalytic and Dielectric Properties, Kansas State University Manhattan, Kansas, 2006.
- [13] J. Li, D. Guo, X. Wang, H. Wang, H. Jiang, B. Chen, *Nanoscale Res. Lett.* 5 (2010) 1063–1071.
- [14] S. Baskoutas, A. F. Terzis, *J. Appl. Phys.* 99 (2006) 013708-1 – 013708-4.
- [15] C. Chen, J. Liu, P. Liu, B. Yu, *Adv. Chem. Eng. Sci.* 1 (2011) 9-14.
- [16] S. Kant, A. Kumar, *Adv. Mat. Lett.* 3 (2012) 350-354.
- [17] F.J. Sheini, J. Singh, O.N. Srivasatva, D.S. Joag, M.A. More, *Appl. Surf. Sci.* 256 (2010) 2110–2114.
- [18] S.J. Pearton, I.E. Fellow, D.P. Norton, M.P. Ivill, A.F. Hebard, M.J. Zavada, W.M. Chen, I.A. Buyanova, *IEEE Trans. Electron Devices* 54 (2007) 1040-1048.
- [19] M. Qamar, M. Muneer, *Desalination* 249 (2009) 535-540.
- [20] M. Faiz, N. Tabet, A. Mekki, B. S. Mun, Z. Hussain, *Thin. Solid. Films* 515 (2006) 1377–1379.
- [21] J. Kim, K. Yong, *J. Nanopart. Res.* 14 (2012) 1033-1 – 1033-10.
- [22] S. Gharibe, L. Vafayi, S. Afshar, *J. Indian Chem. Soc.* 91 (2014) 527-532.
- [23] A.İ. Vaizoğullar, A. Balçı, *Int. J. Res. Chem. Environ.* 4 (2014) 161-165.
- [24] Z.R. Khan, M.S. Khan, M. Zulfequar, M.S. Khan, *Mater. Sci. Appl.* 2 (2011) 340-345.
- [25] R.N. Gayen, K. Sarkar, S. Hussain, R. Bhar, A.K. Pal, *Ind. J. Pure. Appl. Phys.* 49 (2011) 470- 477.
- [26] R.Y. Hong, J. H. Li, L.L. Chen, D.Q. Liu, H. Li, Z.Y. Zheng, *J. Ding, Powder Technol.* 189 (2009) 426–432.
- [27] S. Wang, H. Cao, F. Gu, C. Li, G. Huang, *J. Alloy. Compd.* 457 (2008) 560-564.
- [28] F. Li, X. Huang, Y. Jiang, L. Liu, Z. Li, *Mater. Res. Bull.* 44 (2009) 437-441.
- [29] Y. Li, G. Lu, S. Li, *J. Photochem. Photobiol. A* 152 (2002) 219-228.
- [30] W. Choi, A. Termin, M. R. Hoffmann, *J. Phys. Chem.* 98 (1994) 13669-13679.